Biochimica et Biophysica Acta, 501 (1978) 217—231

BBA 47442

HIGH-ORDER FLUORESCENCE AND EXCITON INTERACTION IN PHOTOSYNTHETIC BACTERIA

MAYFAIR CHU KUNG and DON DEVAULT *

Johnson Research Foundation, University of Pennsylvania, Philadelphia, Pa. 19104 (U.S.A.)

(Received May 24th, 1977)

Summary

We have observed fluorescence at visible wavelengths from chromatophores of photosynthetic bacteria excited with infrared radiation which we attribute to bacteriochlorophyll of the antenna system. The fluorescence is prompt (no delay greater than 5 ns). Its spectrum shows peaks at 445, 530 (broad) and 600 nm when excited with either 694 or 868 nm. Quantum yield is of the order of 10^{-9}. The dependence on intensity indicates generation by mainly third-order processes which could involve triplet states in combination with excited singlets. Second-order single-singlet fusion could also contribute. The high-order fluorescence can also be explained as arising from absorption of a second photon by singlet excited states.

Introduction

In this paper we report the observation of emission of light in the visible region (400—600 nm) when photosynthetic bacteria were excited with laser light of 694 or 868 nm. It appeared first as apparent laser artifact which insisted on coming thru blue filters (Corning 4-96) known to absorb the far-red 694 nm laser light very efficiently. Observation of the pulses with a fast photodiode detector (EG and G SGD-444) plus fast amplifier (overall resolving time, 10 ns) showed no increase in width more than 5 ns over that of the 694 nm exciting pulse (26 ns full width at half maximum). Since the observed photons have up to twice the energy of the absorbed photons it is clear that two or more absorbed photons must contribute to the energy of the emitted photons. As in reaction kinetics we call such a process "higher order" (than first). The nano-

* To whom correspondence should be addressed. Present address: Dept. of Physiology and Biophysics, University of Illinois, Urbana, Ill. 61801, U.S.A.

Abbreviations: Chl, chlorophyll; BChl, bacteriochlorophyll; PSU, photosynthetic unit; MOPS, morpholinopropane sulfonate.

second lifetime is characteristic of singlet excited states. Triplet states could be involved in combination with singlet excited states giving a lifetime controlled by that of the singlets. Exclusively triplet interactions, however, can be ruled out as they would have a lifetime characteristic of triplet states, ordinarily microseconds or longer. Thus it seems proper to call the observed emission "fluorescence", higher order fluorescence, rather than phosphorescence. Preliminary reports have been made in several places [1—3].

Methods

Chromatophores of *Rhodopseudomonas sphaeroides* Ga (carotenoid-containing) mutant, R-26 (carotenoidless) mutant and *Rhodopseudomonas viridis* (contains bacteriochlorophyll *b*) were prepared by French press (14 kN · cm^{-2} or 1360 atm) from anaerobic cultures grown in the light. Concentration of chromatophores used was such that the concentration of BChl was around 2—3 nmol · cm^{-2} of cuvette area so as to diminish reabsorption of the fluorescence by the sample. It was measured from the absorption spectrum of the sample using ϵ_{870} = 100 $mM^{-1} \cdot cm^{-1}$ for *R. sphaeroides* and ϵ_{603} = 20 $mM^{-1} \cdot cm^{-1}$ for *R. viridis*.

The samples were irradiated in a cuvette having 2.25 cm^2 area and 2.0 mm light path. Quartz windows were used as they gave the least amount of visible fluorescence when irradiated with 694 nm laser light. The observation of fluorescence was from the side opposite to that irradiated.

A pulse of 694 nm exciting light having 26 ns full width at half height was provided by a Q-switched ruby laser in a set-up similar to that previously described [4]. 868 nm light was generated by pumping a liquid dye cell transversely with the ruby laser as described by Chance et al. [5]. The dye was a 10^{-4} M solution of 3,3'-diethylthiatricarbocyanine in dimethylsulfoxide. Two Wratten 88A filters were placed in the light path 88 cm from the sample position to remove scattered, unconverted 694 nm laser light. The wavelength of the output of this dye laser, was determined with a monochromator.

It was found that with 694 nm excitation of high enough laser intensity, emission in wavelengths shorter than 694 nm can be obtained from such samples as paper, quartz and plexi-glass. For this reason, the laser intensities used throughout the experiments were kept below a previously determined limit so as to avoid artifacts from fluorescence arising from substances other than the sample of interest. For experiments with 694 nm exciting light a Corning 2-64 dark red glass filter was placed between the sample and the glass prism that directed the laser light to the sample. This removed any fluorescence from the glass prism. The highest laser energy used in experiments with 694 nm excitation was 40 nE · cm^{-2}. Before each experiment, at each wavelength, an empty cuvette was irradiated with laser light of intensity higher or equal to that used in the experiment. The fluorescence from the empty cuvette with 40 nE/cm^{-2} radiation varied with wavelength but was generally 20—30 times smaller than the fluorescence from the bacterial sample. For experiments with 868 nm exciting light, the highest laser intensity used was 89 nE/cm^{-2}. At that intensity the quartz cuvette still did not show any fluorescence at all wavelengths. How-

ever, for construction of the spectra, we used laser intensities of around 16nE · cm^{-2}.

In running the spectra it was important that all points should correspond to the same laser intensity. The method of handling small random variations in excitation intensity was different at various stages of this investigation. For curves B and C of Fig. 1 all data at each wavelength were simply averaged. In the rest of the experiments we used a silicon photo-diode monitor to record the intensity of individual laser pulses. A beam splitter was used to direct about 10% of the laser light to the monitor. The ruby laser was Q-switched with a rotating prism and could give double pulses, about 260 ns apart, at high pumping-flash intensities. The monitor used in Fig. 1 (curve A) and Fig. 4, curve A would integrate the energy of both pulses. The error introduced was probably small since at the pumping intensities used, the second pulse, when it appeared, was considerably smaller than the first. In later experiments (Figs. 2 and 3) the monitor was an SGD-444 (EG and G Co.) fast photodiode and amplifier. Its output, showing individual pulses was recorded on an oscilloscope. The monitor beam was attenuated before detection by a system designed for reproducibility and stability. The signal from the fluorescence detector was delayed by passage through 90 m of coaxial cable so that it appeared on the same oscilloscope sweep, delayed about 430 ns after the monitor signal. The oscilloscope traces were photographed for later measurement. The monitor was calibrated by correlation of its response with the response of a ballistic thermopile placed at the sample position.

Two different detector set-ups were used at different times: (i) interference filters for different wavelengths, + glass filters + photomultiplier and (ii) monochromator + photomultiplier.

The glass filters used with the interference filters consisted of two or three Corning 4-97 and 4-96 blue filters and served to block the laser wavelengths thoroughly. The filter combinations were taped to the photomultiplier with the interference filter next to the photomultiplier and the whole placed in reproducible position against the cuvette window.

The monochromator, when used, was a Bausch and Lomb 250 mm, Catalogue No. 33-86-40. It had two entrance lenses. One at the aperture was about 60 mm from the cuvette and approximately focused points of the sample onto the plane of the slit. The other at the entrance slit focused the aperture onto the internal concave mirror. The photomultiplier (EMI 9592B) was placed approximately at an aperture focus from a lens at the exit slit. Two Corning 4-97 blue filters were taped over the photomultiplier to guard against laser light straying thru the monochromator.

Each interference-filter combination and the monochromator set-up with their detectors had to be calibrated as to their response to light as a function of wavelength. This is especially so in the case of the interference filters which varied considerably in bandwidth and could give a false peak in a spectrum if a single filter were miscalibrated. We did the calibrations in an absolute manner in order to be able to estimate quantum yields. This was done as follows and is described in some detail because the procedure is not routine and interested readers have a right to know where we may have committed errors:

We set up a measureable, monochromatic light-source intended to imitate

the geometric properties of the fluorescence from the sample cuvette. We did this by putting a piece of white paper in the sample cuvette and irradiating it uniformly on the side opposite the detector with monochromatic light from another monochromator using an incandescent lamp. The paper should give an isotropic dispersal of light from the face of the cuvette similar to that of the fluorescence. The illumination being steady, could be measured by slow techniques. For this purpose we used a small 4 mm^2) glass-encapsulated solar cell (Hoffman EA7E1) whose sensitivity to different wavelengths had been calibrated absolutely with a thermopile *. The solar cell was placed immediately behind the sample cell when calibrating interference filters. It was placed at the aperture of the monochromator at a distance 5.27 cm from the sample position when calibrating the monochromator. The solar-cell response to the calibrating light will be designated $W(\lambda)$ ($nE \cdot cm^{-2} \cdot s^{-1}$). The geometric factor relating this response to the intensity of isotropic emission from the cuvette is taken to be:

$$K = 2(1 - l/\sqrt{l^2 + A/\pi})^{-1} \tag{1}$$

where l = distance between solar cell and cuvette (5.27 cm for monochromator, 0.6 cm for filters), and A = cuvette (sample) area (2.25 cm^2). This formula assumes that the solar cell registers oblique rays in proportion to the cross-sectional area of such rays subtended by its active surface, and also approximates the square cuvette face with a circle of equal area. The significance of K is that a sample of area, A, having a density of isotropically emitting sources equal to X $nE \cdot cm^{-2} \cdot s^{-1}$ will produce a flux density at distance, l, equal to (X/K) $nE \cdot cm^{-2} \cdot s^{-1}$. In the case of the monochromator-detector system $K = 158$ and in the case of the filters, 4.7. The solar cell was calibrated with light having normal incidence and probably does not respond to oblique rays as well as assumed in Eqn. 1, which, therefore, probably underestimates K. The error should not be large in the monochromator case since the angles are not large.

The response of the detectors to the calibrating light as a function of its wavelength will be designated R (λ), measured in millivolts deflection of an oscilloscope trace. The band-width of the calibrating light was much narrower than that of the detecting monochromator or of the interference filters. In the case of the monochromator-detector, R was measured at the central wavelength of the monochromator setting and the band-pass was estimated theoretically from the monochromator and grating geometry as a function of slit-widths. We then calculate a sensitivity D (λ) of the monochromator-detector system defined as follows:

$$D(\lambda) = \frac{R(\lambda)}{SW(\lambda)} \tag{2}$$

where, D has units of $mV \cdot mm^{-1} \cdot nE^{-1} \cdot cm^2 \cdot s$, and S = magnitude of the limiting slit-width in the measuring monochromator (1.5 mm).

In the case of interference-filter-glass-filter combinations the whole band-

* Actually there is an uncertainty in the calibration of the solar cell due to three different thermopiles against which it was calibrated having discordant calibrations. The uncertainty could be as much as a factor of 2 and can be cleared up eventually when a reliably calibrated thermopile is available. The order of magnitude of the quantum yield is not affected, nor the shape of the spectra.

width was explored with the calibraing light. It was especially necessary to do this empirically since the closeness of the filters to the cuvette allowed oblique rays to enter. For each filter a sensitivity factor, $C(\bar{\lambda})$, was derived by graphical integration of the following:

$$C(\bar{\lambda}) = \int \frac{R(\lambda)}{KW(\lambda)}\, d\lambda \tag{3}$$

where λ is the calibrating wavelength, $\bar{\lambda}$ is the characteristic wavelength of the particular filter combination (taken as the λ for peak R/KW) and C has the units $mV \cdot nm \cdot nE^{-1} \cdot cm^{-2} \cdot s^{-1}$.

When the fluorescence was measured the oscilloscope trace of the output of the detector was photographed and the area under the pulse was measured and will be designated $P(\underline{\lambda})$ where λ is the wavelength setting of the detector-monochromator or $P(\bar{\lambda})$ in the case of filter combination, $\bar{\lambda}$. The units are $mV \cdot s$.

The monochromator-determined spectrum of Fig. 2 was calculated by:

$$F(\lambda) = \frac{P(\lambda)K}{S_1 S_2 B D(\lambda)} \tag{4}$$

where $F(\lambda)$ is the fluorescence per unit area of sample and per unit wavelength interval as a function of λ in units of $nE \cdot cm^{-2} \cdot nm^{-1}$, S_1S_2 = monochromator slit widths (1.5 mm, 2.5 mm), and B = bandwidth of monochromator per unit slit-width ($6.67\ nm \cdot mm^{-1}$).

The spectra of Fig. 3 were calculated according to:

$$F(\bar{\lambda}) = \frac{P(\bar{\lambda})}{C(\bar{\lambda})} \tag{5}$$

The other spectra shown were calculated in the same way but not absolutely (the photomultiplier voltages for P and R may have been different).

The methanol extract for the experiment shown in Fig. 5 was made by adding cold, degassed methanol to R-26 whole-cell pellets or *R. sphaeroides* Ga chromatophores in the dark. The pellet was washed with 5 ml of methanol three times. The extract was centrifuged to separate the supernatant from the pellet. The pellet was then suspended in 3% Triton, 20 mM MOPS, 100 mM KCl and 1 mM $MgCl_2$ solution. BChl concentration in methanol supernatant was determined on the basis of an extinction coefficient of $60\ mM^{-1} \cdot cm^{-1}$ at 771 nm [6].

Results and Discussion

Fig. 1. shows the fluorescence spectra from *R. sphaeroides* Ga and R-26 chromatophores with 868 nm excitation using the interference-filter detector system. Each spectrum shows a sharp peak at 445 nm, a broad peak around 510—560 nm and a rising slope beyond 590 nm indicating a possible peak. Since the Ga mutant has carotenoids and the R-26 does not, it appears that carotenoids are not involved in this fluorescence. Fig. 2 shows another fluorescence spectrum of *R. sphaeroides* Ga chromatophores, also excited by 868 nm laser light, but in this case the detector system was a monochromator

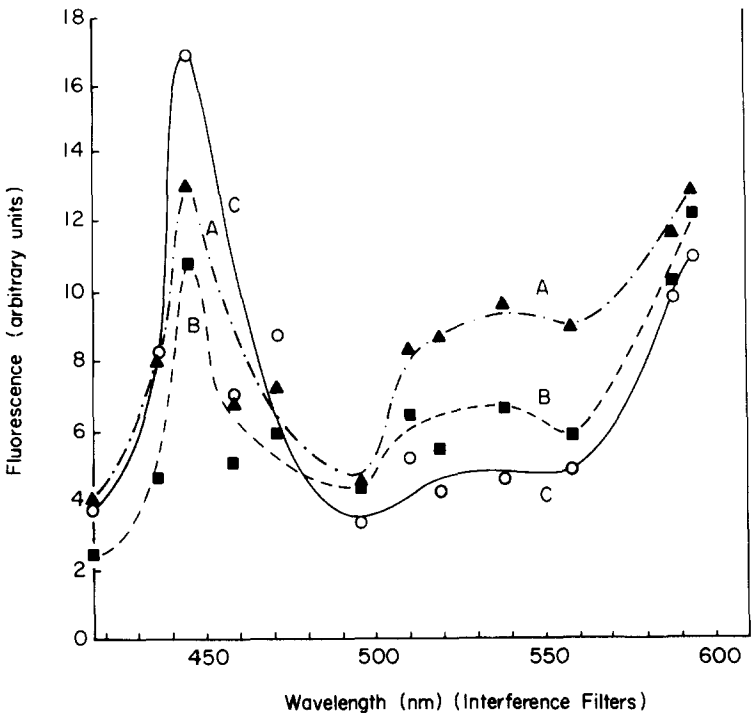

Fig. 1. Fluorescence spectra of *R. sphaeroides*, Ga and R-26 mutants. The exciting light was 868 nm dye laser. (A) ▼, Ga chromatophores: BChl concentration = 1.99 nmol · cm^{-2} (cuvette area), photons adsorbed = 12 nE · cm^{-2}. (B) ■, Ga chromatophores; BChl concentration = 1.96 nmol · cm^{-2}, photons absorbed = 5.9 nE · cm^{-2}. (C) ○, R-26 chromatophores: BChl concentration = 3.7 nmol · cm^{-2}, photons absorbed = 7.0 nE · cm^{-2}. Interference-filter detector system. The vertical scales for the different curves are not related. See Methods for treatment of the data.

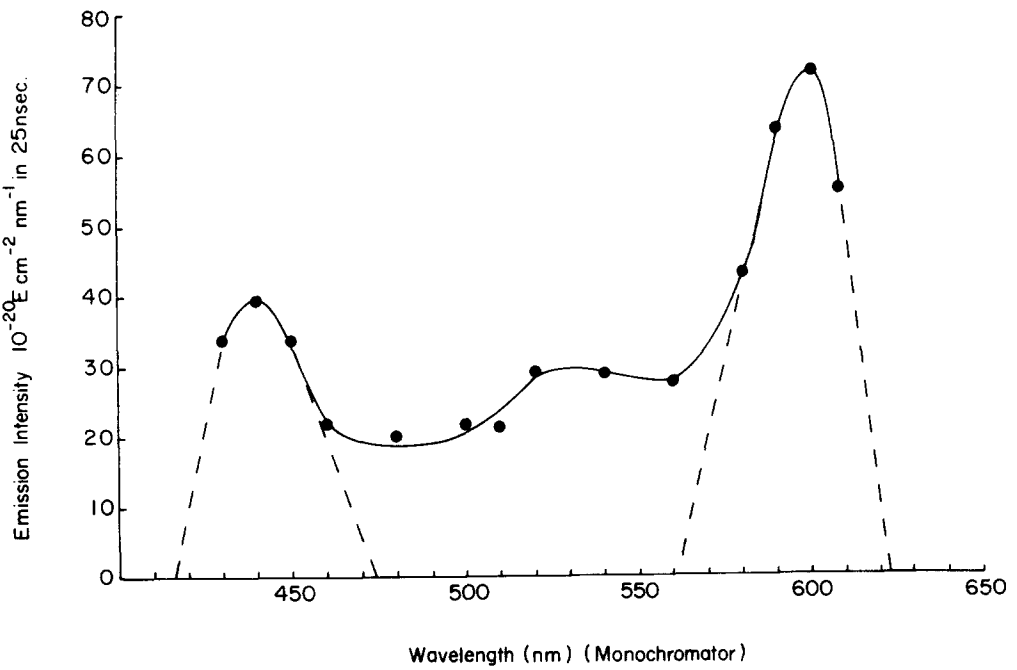

Fig. 2. Fluorescence spectra of *R. sphaeroides* Ga chromatophores excited with 868 nm dye laser. Monochromator detector system. The bandwidth of the monochromator was 16.7 nm. BChl concentration = 2.4 nmol · cm^{-2}, photons absorbed = 10.7 nE · cm^{-2}. The dotted lines map out the areas used in quantum yield determination.

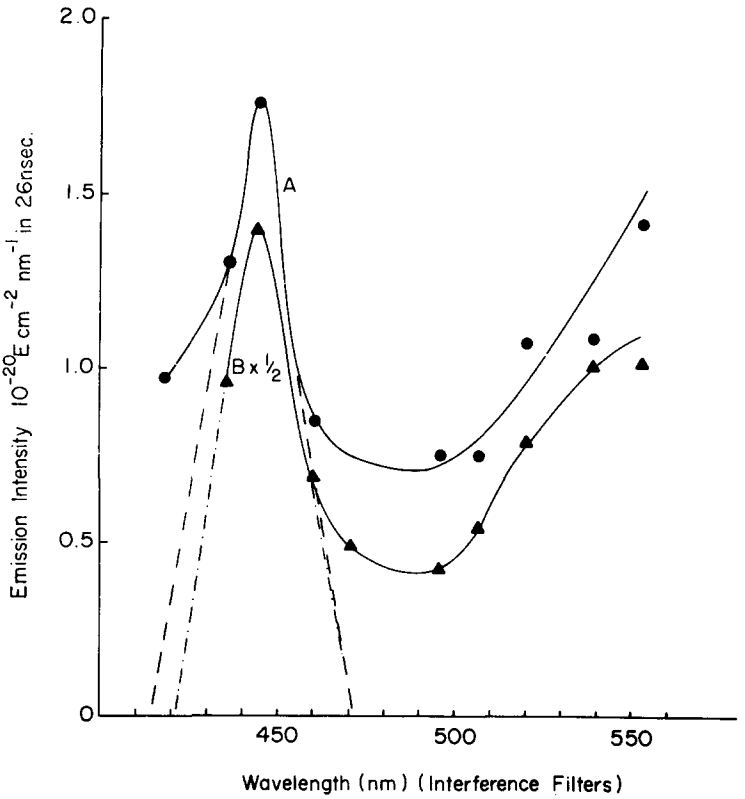

Fig. 3. Fluorescence spectrum of *R. sphaeroides* Ga chromatophores excited by 694 nm ruby light. (A) BChl concentration = 2.0 nmol · cm^{-2}, photons absorbed = 1.6 nE · cm^{-2}. (B) BChl concentration = 2.64 nmol · cm^{-2}, photons absorbed = 2.2 nE · cm^{-2}. Interference-filter detector system. The dotted lines map out the area under the fluorescence peak used in quantum yield determinations.

coupled to the photomultiplier. This spectrum also shows peaks at 440 nm, 520—540 nm and a peak at 600 nm. Fig. 3 shows the fluorescence spectra of *R. sphaeroides* Ga chromatophores excited with 694 nm light and shows a peak at 443 nm. The solid curve in Fig. 4 shows a *R. viridis* fluorescence spectrum when this BChl *b*-containing bacteria was excited with the 868 nm laser. It shows a peak at 445 nm and a broad peak from 520 to 560 nm. The 445 nm peak is, however diminished when compared with the *R. sphaeroides* spectra. These figures show that fluorescence spectra obtained with 868 and 694 nm excitation for *R. sphaeroides* are very similar. The intensities of fluorescence plotted in Figs. 2 and 3 were measured absolutely as explained under Methods and quantum yields were calculated. The results are shown in Table I.

The similarity of the spectra taken with the monochromator and with interference filters gives credence to the calibration of the filters and the monochromator. However, resolution of these spectra are limited by the small number of available filters and the broad band-width used with the monochromator.

Measurements made with an empty quartz cuvette and also with the buffer used to suspend the chromatophores gave very little or no fluorescence at all. Different chromatophore samples prepared by different individuals all exhibit

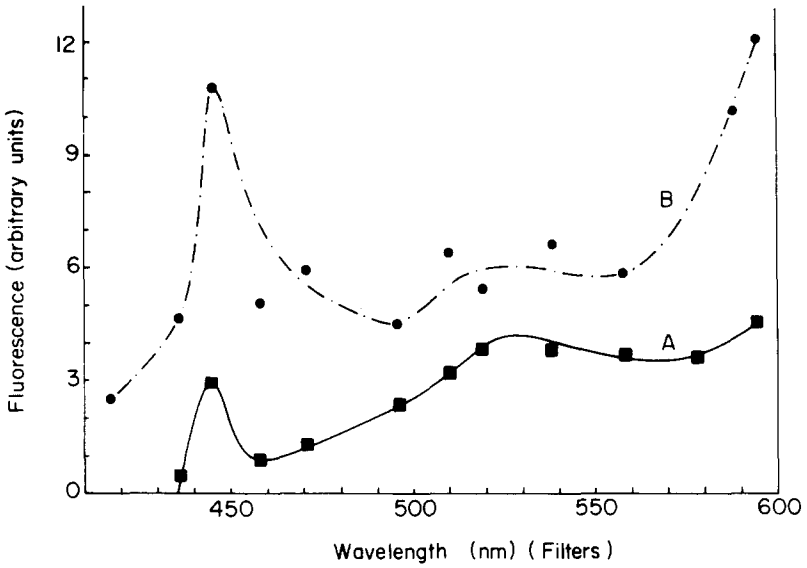

Fig. 4. Comparison of the fluorescence spectra of *R. sphaeroides* Ga chromatophores and *R. viridis* chromatophores. (A) *R. viridis*, BChl *b* concentration = 4.0 nmol · cm^{-2}, photons absorbed = 3.3 nE · cm^{-2}. Interference-filter detector system. Exciting light was 868 nm dye laser. (B) same data as B in Fig. 1. Vertical scales of the two curves not correlated.

this visible fluorescence suggesting that the fluorescing substance is not a random impurity that might vary with method of preparation. If the fluorescence were due to photodegraded pigments in the chromatophores, it should increase with increasing number of laser shots experienced by the sample. This is contrary to experimental observations. We conclude that the fluorescing substance is probably natural to chromatophores.

Fig. 5 shows an attempt to fractionate the chromatophores. Chromatophores of *R. sphaeroides* Ga were treated as described under Methods. The resuspended pellet in buffer/Triton solution and the methanol supernatant containing the pigments both showed no fluorescence with 868 nm excitation.

TABLE I

QUANTUM YIELDS OF HIGH-ORDER FLUORESCENCE FROM *R. SPHAEROIDES*

Data from Fig.	Fluorescence peak (nm)	Excitation λ (nm)	Detector	Incident photons (nE · cm^{-2})	Photons absorbed (nE · cm^{-2})	Emitted photons (nE · cm^{-2})	Quantum efficiency
3B	440	694	Interference filter	38.5	2.2	$7.9 \cdot 10^{-10}$	$3.6 \cdot 10^{-10}$
3A	440	694	Interference-filter	38.6	1.6	$5.1 \cdot 10^{-10}$	$3.2 \cdot 10^{-10}$
2	440	868	Monochromator	25.2	10.7	$1.4 \cdot 10^{-8}$	$1.3 \cdot 10^{-9}$
2	600	868	Monochromator	25.2	10.7	$2.5 \cdot 10^{-8}$	$2.3 \cdot 10^{-9}$
2	400—600	868	Monochromator	25.2	10.7	$6.2 \cdot 10^{-8}$	$5.8 \cdot 10^{-9}$

However, with 694 nm excitation, the pellet suspension showed a fluorescence signal (curve B) whose magnitude was 20—30% of that of the chromatophore sample before extraction (curve C). The pellet suspension was very turbid as compared with the chromatophore sample. Because the intensity is lower and

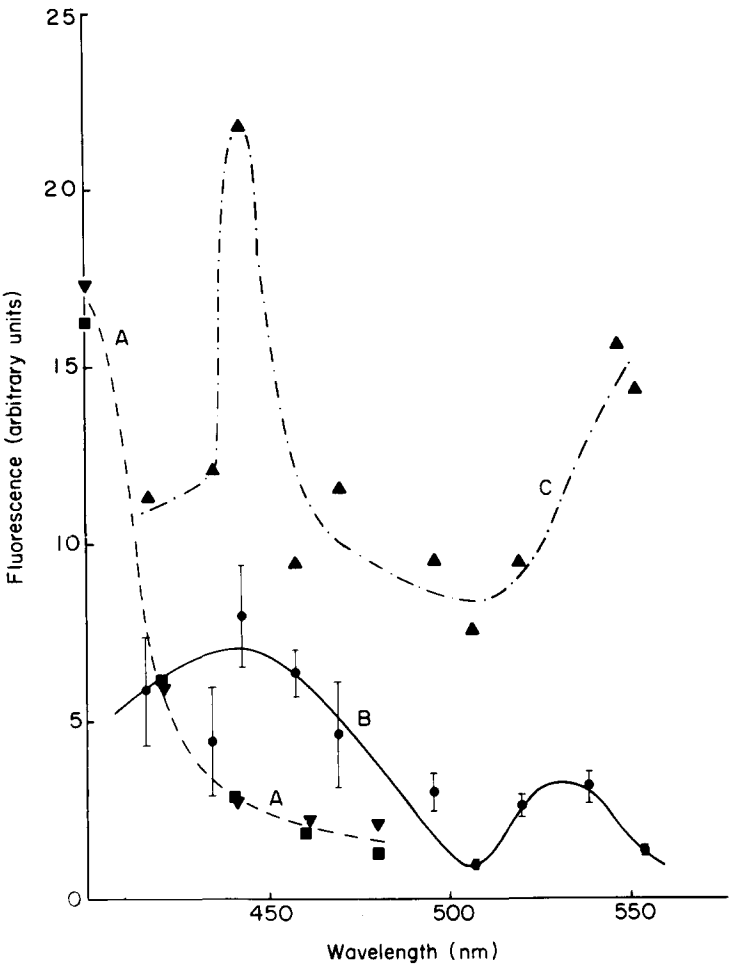

Fig. 5. Fluorescence spectra of chromatophore fractions excited at 694 nm. Variation in laser energy was approximately corrected by dividing the laser energy into the amplitude of fluorescence. (A) Methanol solution of BChl extracted from R-26 (■) and Ga (▼). BChl concentration = 7.6 nmol · cm^{-2}. Monochromator detector system. ■, the sample was discarded after each laser flash, photons absorbed range from 10.1 to 14.7 nE · cm^{-2}. The absorption spectrum of the discarded sample did not show any degraded pigments. ▼, sample was discarded after two shots. Photons absorbed range from 11.8 to 14.7 nE · cm^{-2}. Slight degradation of BChl was observed in the discarded sample as absorption increases around 690 nm. (B) Represents fluorescence from the resuspended pellet of pigment-extracted Ga chromatophores prepared as described under Methods. The concentration of resuspended material was that coming from the same volume of chromatophores with a BChl concentration = 8.8 nmol · cm^{-2}. The suspension was stirred before each laser shot. Incident laser energy ranged from 51.5 to 37.3 nE · cm^{-2}. (C) *R. Sphaeroides* Ga chromatophore. BChl concentration = 3.5 nmol · cm^{-2}, a dilution from the same suspension used for the extraction of A and B, however, the fluorescence readings are multiplied by 8.8/3.5 for comparison on same scale as B. Photons absorbed range from 2.3 to 3.5 nE · cm^{-2}, the incident energy being the same as for B. B and C readings were taken alternately on the same day.

because the turbidity may have enhanced the scattering and because it did not respond to 868 nm excitation, we believe that this fluorescence has nothing to do with that observed from the chromatophores.

Fig. 5 also shows fluorescence from methanol extracts of the pigments from both Ga and R-26 mutants of *R. sphaeroides* (curve A). Both extracts contain the BChl while the Ga extract also contains carotenoids and the R-26 does not. The spectrum of fluorescence is seen to be the same from both, suggesting strongly that it comes from the BChl. In vivo BChl has peak absorption at about 860 nm and absorbs well to 900 nm. When dissolved in methanol the peak shifts to about 770 nm. This could account for the response in vivo to excitation by 868 nm and the non-response in vitro. The first-order fluorescence peaks would be at about 900 nm in vivo and 800 nm in vitro. Second-order fluorescence at half these wavelengths would be at about 450 nm in vivo and 400 nm in vitro. The 450 nm peak seen in Figs. 1—4 agrees with the in vivo prediction while Fig. 5 suggests that the extract may be forming a peak at 400 nm or less.

Other evidence also suggest BChl to be responsible for the visible fluorescence. We found qualitatively that for a fixed number of input 868 nm photons, the fluorescence was much stronger for *R. sphaeroides* than *R. viridis*, consistent with the fact that *R. sphaeroides* has BChl *a* and absorbs strongly at 868 nm, while *R. viridis* has BChl *b* and absorbs very weakly at 868 nm. Similarly for *R. sphaeroides*, Table I shows that the same number of incident 868-nm photons produced much more fluorescence than 694-nm photons and *R. sphaeroides* absorbs much more strongly at 868 than at 694 nm. This again suggests that the fluorescence is related to the absorption spectrum of the BChl. The difference in the quantum yield found with 694 and 868 nm excitation is probably not significant as they were done with different detector systems but can be partly accounted for by the difference in intensity of photon absorption and the non-linear dependence of the fluorescence on intensity. Thus it appears that the species which is responsible for the fluorescence spectra in Figs. 1—3 is BChl *a*.

Fig. 6 shows the dependence of fluorescence intensity on intensity of excitation. As abscissa we chose "excitation rate", I, defined as the number of photons absorbed per s per ground-state molecule. Thus:

$$d(S_1)/dt = I(S_0) \tag{6}$$

where (S_1) is the concentration of excited singlet states and (S_0) of ground-state BChl. I is not uniform over the sample unless the absorption of exciting light is small enough so that its intensity does not vary appreciably over the sample. Under such conditions I is related to I', the incident intensity (einsteins $\cdot$ cm^{-2} $\cdot$ s^{-1}), to I_0, the absorbed intensity (also einsteins $\cdot$ cm^{-2} $\cdot$ s^{-1}) and to I_p the integrated incident intensity of the whole pulse (einsteins $\cdot$ cm^{-2}) as follows:

$$I = 2.3\, I'\epsilon \times 10^3 = I_0/b = 2.3\, I_p\epsilon \times 10^3/\Delta t \tag{7}$$

where ϵ is the molar extinction coefficient of the absorbing species at the wavelength of excitation and b is the area concentration (mol $\cdot$ cm^{-2}) of the absorbing species (ground-state BChl) in the cuvette and Δt is the average or effective width of the laser pulse. For this we take the width at half-height. If I', I_0 and

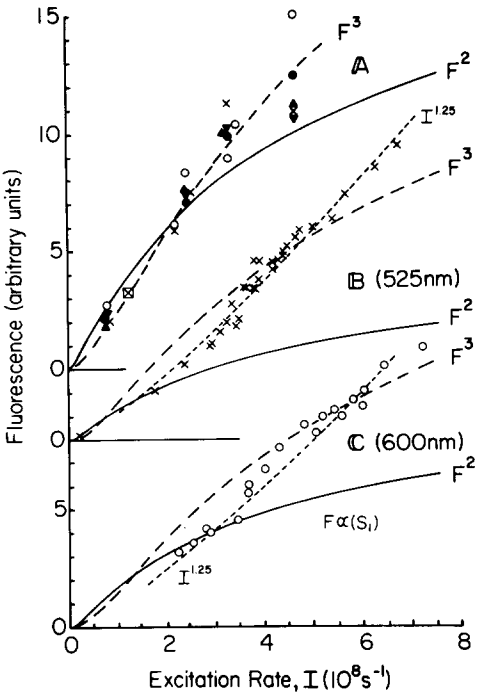

Fig. 6. Dependence of fluorescence measured at different wavelengths on excitation rate, I. Excitation wavelength = 868 nm. Chromatophores of *R. sphaeroides* Ga, BChl concentration = 1.65 nmol · cm^{-2}. Pulse width taken as 25 ns. Interference-filter detection system. (A) Data for various wavelengths as follows: ▲, 445 nm; ▲, 475 nm; X, 525 nm; ●, 545 nm; ○, 600 nm. The vertical scales were adjusted to make point ⊠ common to all wavelengths. Data for "600" nm (○) were obtained with an interference filter that normally had its transmittance maximum at 608 nm but gave a broad transmission from 560 to 600 nm with scattered light. (B) 525 nm. (C) 600 nm. In A, B and C, the solid lines, labelled F^2, are plots of the square of the solid curve in Fig. 7 which fits first-order fluorescence data. Vertical scales adjusted to fit points at low intensity. The dashed lines are proportional to F^3. The dotted lines are proportional to $I^{1.25}$. Both the F^3 and the $I^{1.25}$ plots have vertical scale adjusted to best overall fit to the data.

I_p are evaluated in terms of photons instead of einsteins the corresponding relations are:

$$I = I'\sigma = I_0/nl = I_p\sigma/\Delta t \tag{8}$$

where σ is the absorption cross-section (cm^2 · molecule^{-1}), n is the concentration of absorbing species (ground-state molecules · cm^{-3}) and l is the path length (cm).

The curves of Fig. 6 show a fairly linear dependence on I with a slight conczvity upward. The time available did not allow us to measure the first-order fluorescence which would require infrared techniques. However, for comparison, we have the extensive data of Monger et al. [7] and of Monger and Parson [8] which was gathered under conditions of sample and laser pulse very similar to ours. This data is replotted in Fig. 7 which also includes some from Mauzerall [9,10] on chloroplasts. It is seen that in the same range of excitation the first-order fluorescence falls off drastically from linearity. In fact it can be shown [16] that the fluorescence falls off faster than can be explained by sin-

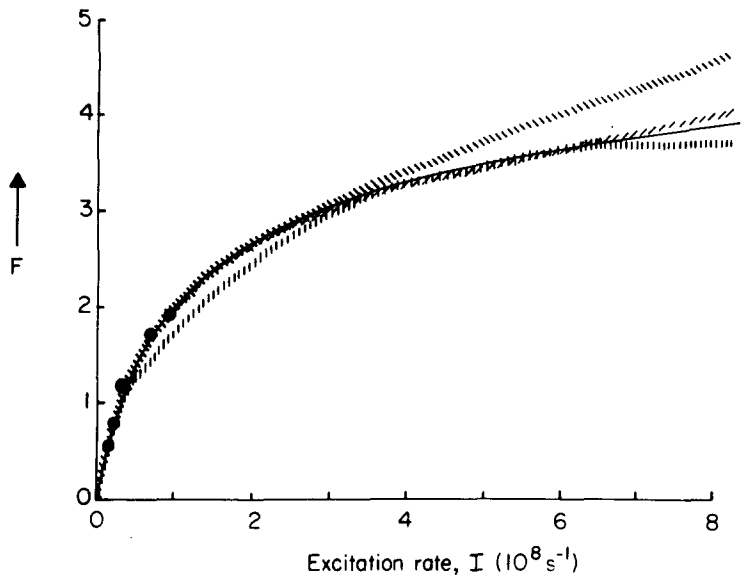

Fig. 7. Dependence of first-order fluorescence on excitation rate. Data on first-order fluorescence yields taken from Monger et al. [7], *R. sphaeroides* (2.4.1) (their Fig. 5) (||||||), Monger and Parson [8] (their Figs. 6A (//////) and 6B (\\\\\\), *R. sphaeroides* (2.4.1) and Ga, resp., and Mauzerall [9,10] *Chlorella* (his Fig. 1) (•), multiplied by their excitation intensities to get fluorescence intensity. The abscissa, I, is figured from Monger et al. [7] by dividing the absorbed intensity given by them by 15 ns, their pulse width, and by $b = 47\ \mu M \cdot cm$. It is figured from Monger and Parson [8] by dividing incident photon intensity given by them by their pulse width, 20 ns, and multiplying by σ estimated from their given BChl concentrations and percent absorptions. The excitation intensity scale used by Mauzerall is X = hits per photosynthetic unit per laser pulse. It is converted to I by dividing by the pulse width, 7 ns, and by N, the number of chlorophyll molecules per photosynthetic unit estimated by him to be 100. His concentrations were so low that only a small fraction of incident light was absorbed (personal communication). The solid curve is Eqn. 9. Vertical scales of data adjusted for best overall fit. Ordinate scale given is in units of F corresponding to calculated curve.

glet-singlet annihilation. A similar non-linear dependence on excitation intensity has been observed in the formation of triplet states of chlorophyll, bacteriochlorophyll and carotenoids. Mathis [11] noticed such a dependence on laser intensity of carotenoid triplet states in chloroplasts and suggested triplet-triplet annihilation as an explanation for the decrease in quantum yield at high intensities. The same phenomenon was noticed earlier in bacteria by Parson [12] and by Seibert and DeVault [13] without understanding that carotenoid triplets were involved until so diagnosed by Cogdell et al. [14]. Monger et al. [7] measured the dependence on laser intensity again and suggested singlet-triplet fusion as the cause for decrease of quantum yield of BChl triplets, of carotenoid triplets and of fluorescence. Mauzerall [9,10] and Campillo et al. [15] both measured a falling off of quantum yield of fluorescence from *Chlorella* with increasing excitation intensity. Mauzerall suggested a model in which photons hitting a photosynthetic trap after the first hit are destroyed without fluorescing while Campillo et al. [15] suggested singlet-singlet annihilation.

In Fig. 7 the ordinate, labelled F, applies to the solid curve which is calcu-

lated according to the equation:

$$F = (1 + C/D) + \sqrt{(1 + C/D)^2 + C} \tag{9}$$

where $C = 1.33 \cdot 10^{-7}\ I$, and $D = 10$. For present purposes we may regard Eqn. 9 as empirical, fitting the first-order data as shown. F is thus proportional to the concentration of singlet excited states.

In Fig. 6 the curves labelled F^2 and F^3 are proportional to the squares and cubes, respectively, of F as given by Eqn. 9. For the F^2 curves the proportionality constant was chosen for best fit at low excitation intensity. The F^3 curves were given best over-all fit to the data. Also shown in Fig. 6 are curves which are proportional to $I^{1.25}$ with ordinates adjusted for best over-all fit. The data of part A (Fig. 6) might give a tolerable fit to F^2. However, the other data definitely do not fit F^2. All three parts fit F^3 fairly well and parts B and C (Fig. 6) are even better fitted by $I^{1.25}$. The conclusion from this is that if the higher order fluorescence is the result of exciton interactions they are probably at least third-order. A more thorough analysis will be given in another paper [16]. In it we take account of possible singlet-triplet interactions. We use data from Monger and Parson [8] which indicate that triplet state concentrations under conditions similar to ours are approximately proportional to $I^{0.40}$ in the range of I with which we are concerned. In the same range the first-order fluorescence is approximately proportional to $I^{0.42}$. Curves B and C of Fig. 6 are found to fit $I^{1.35}$ and $I^{1.30}$ even better than $I^{1.25}$. Various combinations of possible singlet and triplet interactions will give exponents adding approximately to these.

Several people have suggested that we consider two-photon absorption processes. We tended to rule these out on the basis that excitation by 868 nm gives the same results as excitation by 694 nm (compare Fig. 3 with Figs. 1 and 2). At the urging of Professor R.M. Hochstrasser we reconsider the idea with his suggestion for successive photon absorptions:

$$S_0 \xrightarrow{I_1} S_1 \; *\rightsquigarrow \; S_1 \xrightarrow{I_2} S_n \; *\rightsquigarrow \; S_n \longrightarrow \text{Fluorescence}$$
$$\qquad\qquad\qquad\qquad\qquad\qquad\qquad\qquad\qquad\qquad\qquad\qquad\qquad\qquad\qquad\qquad \rightsquigarrow \text{Relaxation}$$

The S's represent various singlet states of BChl. S_1* and S_n* are higher excited states relaxing rapidly to S_1 and S_n, respectively. These allow different excitation wavelengths to give finally the same states. I_1 and I_2 are the incident photon flux multiplied by absorption cross-sections for ground state and first excited singlet state, respectively (See Eqns. 7 and 8). In the steady-state during a laser pulse the concentration of S_n and, therefore, the intensity of higher-order fluorescence should be proportional to I_2 and to the concentration of S_1. I_2 is proportional to I and $[S_1]$ is proportional, as we have already said, to $I^{0.4}$ in the range of interest. This would make the fluorescence proportional to $I^{1.4}$ which is in fair agreement with the data of Fig. 6. On the basis of present data we must, therefore, consider two-photon absorption as another possible explanation. This process would be accompanied by whatever exiton annihilations are necessary to yield $[S_1]$ proportional to $I^{0.4}$.

The meaning of the near-linearity of the curves of Fig. 6 is that the processes producing this fluorescence or other processes with the same power depen-

dence on I (such as the corresponding radiationless decay paths) must be the principle mode of excitation decay in the range of interest. Any group of processes which have the same power dependence on I and which nearly monopolize the decay paths would have to show linear dependence on I because the total decay rate must equal the excitation rate. This assumes we have approximately steady-state conditions during the laser pulse. This seems reasonable with regard to the singlet states because their lifetimes are short compared to the width of the laser pulses.

The quantum yields ($\approx 10^{-9}$) shown in Table I are reasonable as one expects the radiationless decays from higher excited states to be much faster than radiation.

It is tempting to try to identify the peaks in the spectra of Figs. 1—4 with transitions observed in absorption. We expect the corresponding absorption peaks to occur at up to 20—30 nm shorter wavelengths. We don't know anything to which the 530 nm, (broad) peak could relate. However, the 600 nm peak is close to the 590 nm absorption, 1_A—1_{Qy} [17] and the 445 nm peak might correspond to a shoulder on the 375 nm absorption band. This shoulder is seen in solution to shift from 390 to 440 nm depending upon the solvent [18—20]. Perhaps our 530 nm band represents emission from a virtual state formed during collision between excitons and the broadness might represent an indefiniteness in the conditions of collision.

In summary we have reported a new way of probing the higher excited states of molecules: Observation of emission at wavelengths shorter than that of the exciting light. This method is free from the usual difficulty encountered with such studies. As pointed out by Hochstrasser and McAlpine [21] weak emission observed by direct excitation in the ultraviolet of a molecule to states higher in energy than the first excited state is often not really emission from the higher excited state but is emission from the first excited state of some impurity that absorbs strongly at the excitation wavelength. In this paper we have demonstrated emission from higher excited state of BChl populated through exciton-exciton annihilation, or through second photon absorption.

Acknowledgements

The authors wish to thank Dr. P.L. Dutton and his coworkers for the samples of *R. sphaeroides* and some of the chromatophores. A number of people, among whom may be mentioned M. Gouterman, D. Mauzerall, W.W. Parson, P.A. Loach, Govindjee, K.J. Kaufmann, C.E. Swenberg, and R.M. Hochstrasser have contributed helpful discussions. Mr. D. Henderson helped with the apparatus. We also thank Dr. William Parson for sending us several of his manuscripts before publication. Financial support came from the National Science Foundation (grants PCM76-15724 and PCM76-23744).

References

1 DeVault, D. (1976) Remarks in Brookhaven Symposium No. 28; Chlorophyll-Proteins, Reaction Centers, and Photosynthetic Membranes (Olson, J.M. and Hind, G., eds.), p. 211, Brookhaven National Laboratories, Upton, N.Y.

2 Kung, M.C. and DeVault, D. (1977) Biophys. J. 17, 148a (Abstr. TH-AM-F7)

3 Kung, M.C., DeVault, D. and Chance, B. (1977) Bull. Am. Phys. Soc. 22, 96 Abstr. JI8
4 DeVault, D. (1964) in Rapid Mixing and Sampling Techniques in Biochemistry (Chance, B., Eisenhardt, R.H., Gibson, Q.H. and Lonberg-Holm, K.K., eds.) pp. 165—174, Academic Press, New York
5 Chance, B., McCray, J.A. and Bunkenburg, J. (1970) Nature 225, 705—708
6 Loach, P.A., Banbara, R.A. and Ryan, F.J. (1971) Photochem. Photobiol. 13, 247—257
7 Monger, T.G., Cogdell, R.J. and Parson, W.W. (1976) Biochim. Biophys. Acta 449, 136—153
8 Monger, T.G. and Parson, W.W. (1977) Biochim. Biophys. Acta 460, 393—407
9 Mauzerall, D. (1976) Biophys. J., 16, 87—91
10 Mauzerall, D. (1976) J. Phys. Chem. 80, 2306—2309
11 Mathis, P. (1969) in Progress in Photosynthesis Research (Metzner, H., ed.), Vol. II, pp. 818—822, Tübingen
12 Parson, W.W. (1968) Biochem. Biophys. Acta 153, 248
13 Seibert, M. and DeVault, D. (1971) Biochim. Biophys. Acta 253, 396—411
14 Cogdell, R.J., Monger, T.G. and Parson, W.W. (1975) Biochim. Biophys. Acta 408, 189—199
15 Campillo, A.J., Shapiro, S.L., Kollman, V.H., Winn, K.R. and Hyer, R.C. (1976) Biophys. J. 16, 93—97
16 DeVault, D. and Kung, M.C. (1977) Photochem. Photobiol., in the press
17 Platt, J.R. (1956) in Radiation Biology (Hollaender, A., ed.), Chapter 2, p. 83, McGraw-Hill Book Co., New York
18 Parson, W.W. and Cogdell, R.J. (1975) Biochim. Biophys. Acta 416, 105—149
19 Connolly, J.S., Gorman, D.S. and Seely, G.R. (1973) Ann. N.Y. Acad. Sci. 206, 649—669
20 Weiss, Jr., C. (1972) J. Mol. Spectrosc. 44, 37—80
21 Hochstrasser, R.M. and McAlpine, R.D. (1966) J. Chem. Phys. 44, 3325